Journal of the Oceanographical Society of Japan
Vol. 35, pp. 179 to 186, 1979

Discussion on the Critical Wind Speed for Wind-Wave Generation on the Basis of Shear-Flow Instability Theory*

Sanshiro KAWAI**

Abstract: Observed critical wind speeds for the generation of wind waves are compared with those derived from a shear-flow instability theory. The theory predicts that the critical wind speed depends on the fetch and, for the case of infinite fetch, it is 93 cm s^{-1} at 30 cm above the mean water surface, which agrees well with observations at sufficiently large fetch. For water containing soap, the much larger critical wind speeds which are observed cannot be explained by the reduction of surface tension alone. A qualitative discussion suggests that the elasticity of surface films of soap can effectively increase the critical wind speed.

1. Introduction

It has been shown recently both experimentally and theoretically that wind waves are initiated by a shear-flow instability mechanism (KAWAI, 1979). The same theoretical model is also capable of predicting the critical wind speed for wind-wave generation. The present article is aimed at comparing the observed critical wind speed with that predicted by the theoretical model.

Observational determination of the critical wind speed is not so definite, as theoretical one. Hence, its observed value has some uncertainty, as most observers have noted. Despite this, no one can deny that the actual critical wind speed is far smaller than the value of 6.6 m s^{-1} predicted by the Kelvin-Helmholtz instability theory. Typical values observed so far are 3.3 m s^{-1} (KEULEGAN, 1951) and 2.4 m s^{-1} (KUNISHI, 1957) for laboratory cases and 1.1 m s^{-1} (JEFFREYS, 1924) and 2 m s^{-1} (VAN DORN, 1953) for field cases. The disagreement between these values might be attributable to differences in experimental conditions, as well as to differences in the definition of 'critical wind speed'. In particular, the observation heights of wind speed are not necessarily the same. Among these experiments, Kunishi's (1957, 1963) is the most suitable for the comparison of observed critical wind speeds with those predicted by the present theoretical model, since the experimental conditions, especially the shear-flow profile in air and water, were described in detail. The comparison and discussion will be made in Sections 2 and 3, respectively.

Another subject to be studied in this paper is the extreme increase in critical wind speed when soap is added to the water. According to KEULEGAN (1951) and VAN DORN (1953), the maxima of the critical wind speeds for soapy water are 12 m s^{-1} and 6 m s^{-1}, respectively. It should be noted that they made the measurements under the same experimental conditions as they used for ordinary water. Therefore, the reason for the extreme increase in critical wind speed must lie in the changes in the physical properties of water due to the addition of soap. The physical properties of water pertaining to the present theoretical model are density, viscosity and surface tension (KAWAI, 1979). The amount of soap required to give a significant increase in critical wind speed is not so much as to change appreciably the density and viscosity of the water. On the other hand, the surface tension of soapy water is considerably less, even if the soapy water is very dilute. Therefore, the reduction of surface tension will be investigated as a possible factor relating to the increase of critical wind speed. If a different surface tension is assumed in the present theoretical model, some changes occur in the dispersion relation and consequently in

* Received Apr. 27, revised Nov. 22 and accepted Nov. 26, 1979.

** Geophysical Institute, Faculty of Science, Tohoku University, Sendai 980, Japan

the stability curve that determines the critical wind speed. The wavelengths of the initial wavelets are so short (KAWAI, 1979) that the dispersion relation is strongly controlled by surface tension. Therefore, the critical wind speed might be altered to a large extent.

Besides surface tension, we consider other physical properties related to the surface films formed by the adsorption of the solute to the surfaces. The effects of the surface films have been discussed by many investigators since REYNOLDS (1880). MILES (1967) expressed their effects systematically in terms of three physical properties: (1) the surface elasticity, (2) the surface viscosity and (3) the solubility of the surface material. According to MILES (1967), surface films cause an extreme increase in the damping rate of surface waves. Therefore, surface films are also expected to increase the critical wind speed. In Section 4, we will examine the possible effects of surface tension and surface films on critical wind speed.

Detailed descriptions of the theoretical model, its formulations and the numerical scheme to solve them are wholly omitted in the succeeding sections, since they are identical to those in KAWAI (1979). In short, the model predicts the temporal growth rate β_t and the phase velocity c for a given wave number k of perturbation wave of infinitesimal amplitude, when the shear-flow pattern in the air and water is known.

2. Comparison between observed and predicted critical wind speeds

The experiment by KUNISHI (1957, 1963) was performed in a wind-wave tunnel 75 cm wide, 21.6 m long and 100 cm high, with water up to a depth of 50 cm. The two main factors measured were the air flow profile in the steady state and the time sequence of the developing water flow profile driven by the wind. These measurements were taken at a fetch of about 7.5 m. The number of experimental cases was six (Table 1). In the table, $U_{0.3}$ represents the wind speed at 30 cm above the still water level and u_* the friction velocity of air. In the following discussion, u_* will be used to represent the wind conditions and will be referred to as 'wind speed'. Among the six cases, wind waves were observed only for the case of the highest

Table 1. Wind conditions of the experiment by KUNISHI (1957).

	I	II	III	IV	V	VI
$U_{0.3}$ (cm s^{-1})	54	73	94	109	170	277
u_* (cm s^{-1})	2.3	3.1	4.2	4.7	6.8	10.3
waves	no	no	no	no	no	appear

wind speed. These waves appeared about a hundred seconds after the onset of wind. The wave height was about 1 mm. On the basis of these observations, KUNISHI (1957) reported the critical wind speed $U_{0.3\,\mathrm{crit}}$ as 2.4 m s^{-1}.

As stated in the previous section, detailed measurements of the shear-flow profile in the air and water were made by KUNISHI (1957). The air flow was aerodynamically smooth. As a functional form to represent the smooth flow profile, we will use a modified form of the pattern proposed by MILES (1957), in which the wind speed U at the height y is represented by

$$U(y)=(u_*^2/\nu)y+U_0, \text{ for } 0\leqslant y\leqslant y_1 \qquad (1)$$

in the viscous sublayer and by

$$U(y)=U_1+(u_*/\kappa)\left(\alpha-\tanh\frac{\alpha}{2}\right)+U_0 \quad \text{for } y_1\leqslant y \qquad (2)$$

outside this sublayer, where α is determined by

$$\sinh\alpha=(2\kappa u_*/\nu)(y-y_1) \qquad (3)$$

κ is the von Kármán constant with a constant value of 0.4, y_1 the thickness of the viscous sublayer, U_1+U_0 the velocity at $y=y_1$, U_0 the surface velocity, u_* the friction velocity of air and ν the molecular kinematic viscosity of air. The surface velocity U_0 is related to the water flow discussed later. A nondimensional parameter r for the thickness of the viscous sublayer, defined by

$$r\equiv y_1u_*/\nu=U_1/u_* \qquad (4)$$

remains to be decided. The calculations are made for two wind profiles represented by $r=5$ and 8. Most of the profiles observed by KUNISHI (1957) lie between these two profiles. These expressions of the air flow profile are identical to those of KAWAI (1979).

As for the flow pattern in water, KUNISHI (1957) reported the following functional form;

$$U(y)=U_0[\exp(-\xi^2)+\sqrt{\pi}\,\xi\{1+\Phi(\xi)\}] \quad \text{for } y\leqslant 0 \qquad (5)$$

where the surface velocity U_0 is expressed by

$$U_0=\frac{2}{\sqrt{\pi}}u_{*w}^2\sqrt{\frac{t}{\nu_w}} \qquad (6)$$

ξ is the dimensionless vertical coordinate defined by

$$\xi=\frac{y}{2\sqrt{\nu_w t}} \qquad (7)$$

Φ the error function defined by

$$\Phi(\xi)=\frac{2}{\sqrt{\pi}}\int_0^{\xi}\exp(-x^2)dx \qquad (8)$$

t the time from the onset of the wind, ν_w the molecular kinematic viscosity of water and u_{*w} the friction velocity of water. Since the shearing stress must be continuous at the surface, there is a relation between the two friction velocities,

$$\rho u_*^2=\rho_w u_{*w}^2 \qquad (9)$$

where ρ and ρ_w are the densities of air and water, respectively. Equality (9) was also examined by KUNISHI (1957). These expressions of the water flow are essentially identical to those of KAWAI (1979).

Although these flow patterns are time-dependent, computations are performed under the assumption of a quasi-steady state. The effect of this assumption on the computational results is negligible, as discussed by KAWAI (1979). In the present calculation, the time t in equations (6) and (7) is taken as the time when the observed flow profile in the experiment by KUNISHI (1957) begins to deviate from the functional form (5). The above arbitrary choice of the time t has little effect on the stability curve or the relation between the growth rate and the wavelength of perturbations (KAWAI, 1979).

In Fig. 1 the relationship between the temporal growth rate of amplitude β_t and the wavelength L of perturbation waves, is shown for the case $r=5$. The curves for the four higher wind speeds are from KAWAI (1979). The portion close to the neutral condition ($\beta_t=0$) in Fig. 1 is enlarged in Fig. 2, for a detailed ex-

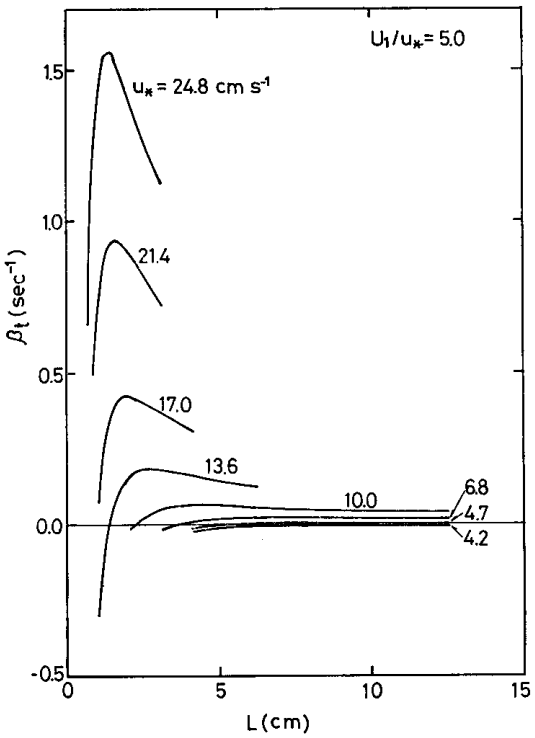

Fig. 1. Stability curves for various friction velocities u_* of air, for the case of $r=5$.

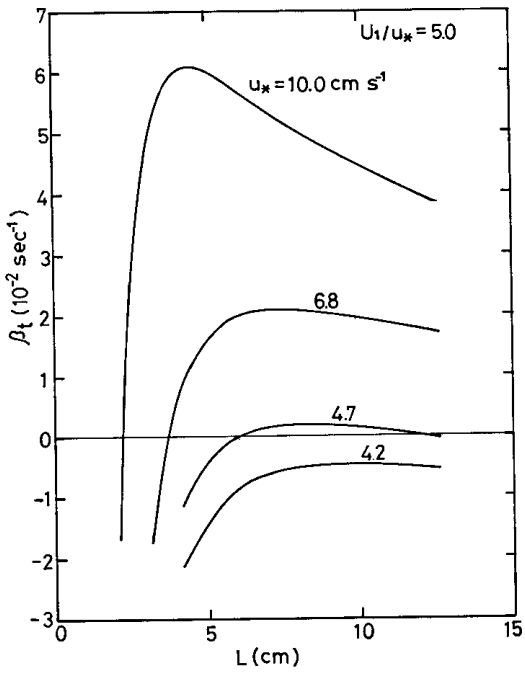

Fig. 2. Enlargement of Fig. 1.

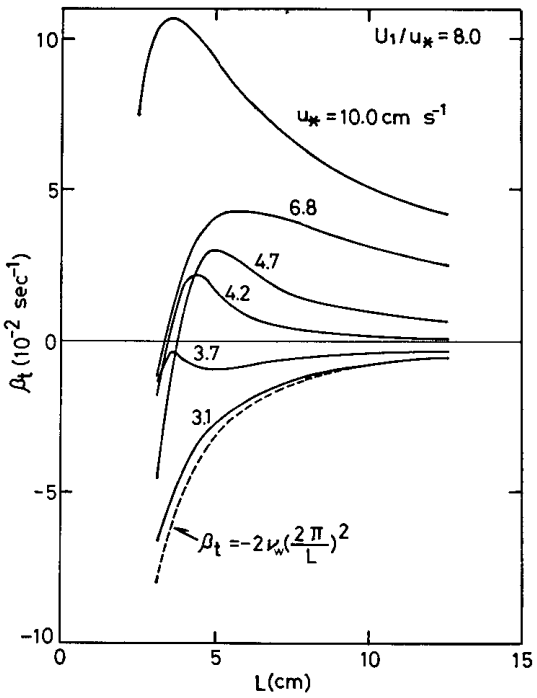

Fig. 3. Stability curves for various friction velocities u_* of air, for the case of $r=8$. Dashed line represents the damping rate caused by the viscosity of water.

amination of the critical wind speed. The theoretical value of the critical wind speed is defined as the minimum wind speed for which the corresponding stability curve has no positive growth rate for any wavelength. The critical wind speed (u_*) for the present case lies between 4.7 cm s^{-1} and 4.2 cm s^{-1}. Regarding the stability curves for the case $r=8$ (Fig. 3), the non-monotonous variation of curves makes it necessary to include an additional curve for $u_*=3.7$ cm s^{-1} in order to make a detailed examination of the critical wind speed. The dashed curve represents the damping rate given by LAMB (1932) for the particular case when mean motion in the air and water vanishes. The stability curves approach the dashed curve asymptotically, as the air flow approaches zero. For this case of $r=8$, the critical wind speed (u_*) lies between 4.2 cm s^{-1} and 3.7 cm s^{-1}.

Before comparing the theoretical results with the observations of KUNISHI (1957), let's examine the results of MILES (1962) in which similar stability curves were obtained in a somewhat different manner. Although the critical wind speed was not clearly distinguished by MILES, the diagrams in MILES seem to show that the critical wind speed $u_{*\,\mathrm{crit}}$ is smaller than 6 cm s^{-1} and 4.5 cm s^{-1}, respectively, for the case of $r=5$ and $r=8$. These values are consistent with the present results. The non-monotonous behavior of the stability curves as in Fig. 3 was explained by MILES (1962), as a resonance phenomena between the surface waves in which we are interested, and Tollmien-Schlichting waves. The resonance conditions for the case of $r=8$ are $u_*=4.5$ cm s^{-1} and $L=4.7$ cm (MILES, 1962). Although these values are nearly equal to those of the present case, the present growth rate is much smaller than that of MILES (1962). For the case of $r=5$, Miles' (1962) diagrams showed the occurrence of resonance at $u_*=4.8$ cm s^{-1}, but the present results differ remarkably from Miles' in the monotonous nature of the stability curves. With an analysis similar to that of the present paper, VALENZUELA (1976) also reported monotonous stability curves, for $r=5$. Hence, the discrepancy between the present results and Miles' (1962) can be interpreted as due to some inadequate assumptions in the analysis by MILES (1962), as pointed out by VALENZUELA (1976) and TAKEMATSU (1978).

Table 2. Critical wind speed predicted by the present theoretical model.

	$u_{*\,\mathrm{crit}}$ (cm s^{-1})	$U_{0.3\,\mathrm{crit}}$ (cm s^{-1})	$U_{10\,\mathrm{crit}}$ (cm s^{-1})
$r=5$	4.5	93	133
$r=8$	4.0	93	129

In any case, it is shown that theoretical value of the critical wind speed is much smaller than the values observed by KUNISHI (1957), as shown in Table 2. In the table, $U_{0.3\,\mathrm{crit}}$ and $U_{10\,\mathrm{crit}}$ represent the critical wind speeds at the heights of 30 cm and 10 m, respectively. They are computed from $u_{*\,\mathrm{crit}}$ by use of the above functional form for the air flow. In the next section, a discussion will be given of the reason for the above discrepancy.

3. Interpretation of the discrepancy between predicted and observed values of the critical wind speed

The critical wind speed predicted by linear instability theories such as the present one signifies that, for higher wind speeds than the

critical one, there is a range of wavelengths where any perturbations, however small they are, grow exponentially with time. On the other hand, some perturbations of finite amplitude may grow with time, even if the wind speed is smaller than the critical value. In this connection, it may seem strange that in the experiments by KUNISHI waves were not generated even when positive growth rates are expected from the linear theory. However, this discrepancy may be accounted for by the fact that the present theory assumes a spatially homogeneous field. The real process in the experiments by KUNISHI (1957) does not necessarily fulfill this condition, as will be shown later.

For the five cases of lower wind speeds in the experiment by KUNISHI (1957), waves did not appear, even after the wind blew for 100 seconds or more. In the later stage of the process, effects of the windward coast cannot be neglected. Then, spatially growing waves must be considered, rather than temporally growing ones. A steady field may attain after so long a time. According to GASTER (1962), the spatial growth rate β_x and the temporal growth rate β_t are related to each other by

$$\beta_x=\beta_t/c_g\,, \qquad (10)$$

where c_g represents the group velocity of the perturbation waves. Since the group velocity is positive in the present problem, the sign of the growth rate remains unaltered by conversion (10). Therefore, the conversion itself cannot solve the above discrepancy between the predicted and observed values of the critical wind speed, since the former value is decided by the sign of the growth rate. However, the discrepancy can be cleared up to some extent, if the finiteness of the fetch in the experiment is taken into account, as discussed below.

If we express the amplitude of disturbance waves at $x=0$ with a_0, then the amplitude $a(x)$ at a fetch x is expressed by,

$$a(x)=a_0\exp(\beta_x x) \qquad (11)$$

Even if the growth rate β_x is positive, the perturbation waves cannot be measured and the situation is judged as of 'no wave', if the amplitude (11) is smaller than the lower limits of the measuring device. Thus, the critical wind speed at a finite fetch can be greater than that expected from the present theory.

Let's discuss further the equation (11) under two assumptions: (1) the initial disturbance a_0 is constant and (2) the lower limits of the measuring device are constant. When a positive growth rate β_x is given, (11) indicates the ex-

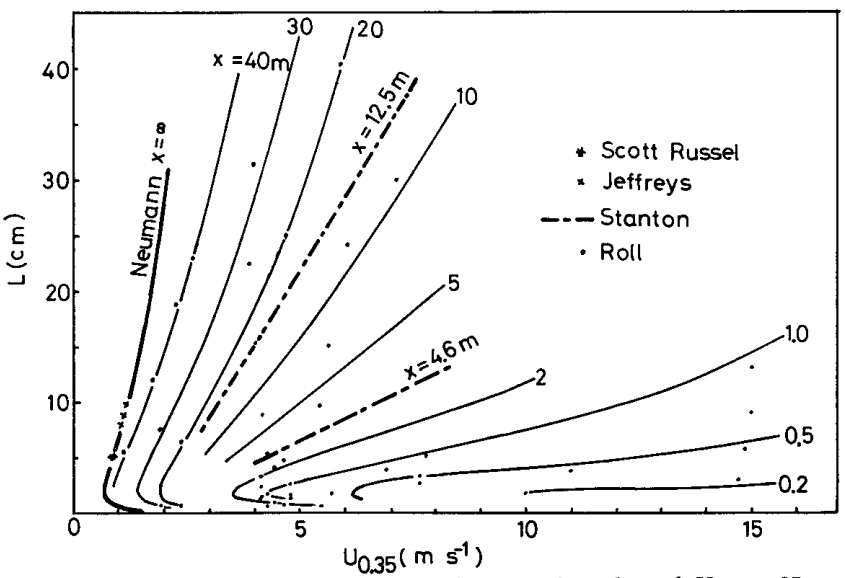

Fig. 4. Wavelengths L of observed waves as a function of wind speed $U_{0.35}$ at 35 cm above water surface and of the observed fetch x. Isopleths are drawn, based on the observed values shown with various symbols. A reproduction of Roll's figure (1951: fig. 2).

istence of a critical fetch; no wave is detectable for fetches smaller than the critical value. Since β_x depends on the wind speed, the critical fetch also depends on it. This is the case in Fig. 4, which is a reproduction of Roll's figure (1951: fig. 2), where the wavelengths of the observed waves were shown as a function of the observed fetch as well as the wind speed $U_{0.35}$ at a height of 35 cm. When a fetch is fixed in the figure, the minimum wind speed required for the appearance of waves can be designated, and for a fixed wind the minimum fetch can be designated in the same manner. Thus, these observational results support the existence of the critical fetch, despite a lack of strict assurance that the above two assumptions are fulfilled in these observations. This might show that actual conditions do not extremely deviate from the two assumptions, if observations are made with the naked eye under natural wind conditions, as those observations in the figure were.

Next, an ideal case of infinite fetch is discussed. In this extreme, the critical wind speed predicted by the theory of temporally growing waves should coincide with that of the spatially growing ones, as expected from equations (10) and (11). On the other hand, if we attend only to the original data (not to the smooth curves) in Fig. 4, the minimum wind speed for the appearance of waves is about 90 cm s^{-1}, which corresponds to the case of virtually infinite fetch. If we adopt this value of the minimum wind speed as the observed critical wind speed at a sufficiently large fetch, it is consistent with the theoretical value listed in Table 2. The minimum wind speed along the smooth curve for the infinite-fetch case in the figure is about 70 cm s^{-1}. However, it appears inadequate to adopt it as the critical wind speed, since no observations were made near the critical value and the smooth curve was drawn under the assumption that the wavelength of the most preferred waves is 1.7 cm, as stated by ROLL (1951). There is no firm base for this assumption. Moreover, it conflicts with the present results shown in Figs. 1 to 3. Hence, the above adoption of the value $U_{0.35\ \mathrm{crit}}=90$ cm s^{-1} as the observed critical wind speed at a sufficiently large fetch seems more reasonable.

In conclusion, the critical wind speed depends on the fetch, and the present model predicts it as $U_{0.3\ \mathrm{crit}}=93$ cm s^{-1} ($U_{0.35\ \mathrm{crit}}=95$ cm s^{-1}) for the infinite-fetch case which is in close agreement with observations.

4. The critical wind speed for soap-water case

Two speculations were made on the cause of the increase of the critical wind speed for the case of soapy water, in Section 1. The first involved the reduction of surface tension and the other the formation of surface films. The two phenomena have the same cause, that is the adsorption of solute to the surface. Therefore, it is impossible experimentally to isolate these two kinds of change in the physical properties of the fluid. But it is possible for the theoretical model to analyze them separately.

First, the effect of the reduction of surface tension will be analyzed. Fig. 5 shows the stability curves near the critical wind speed, corresponding to the case when the surface tension is reduced to half that of ordinary water, for the case $r=5$. The other conditions are identical to those of ordinary water. These stability curves are nearly the same as those in Fig. 2, and no significant change in critical wind speed is seen. As a result, it is concluded that physical properties of the surface films described in Section 1, have to be taken into account, in order to explain the extreme increase of the critical wind speed.

As stated in Section 1, MILES (1967) proposed a model to analyze the effect of surface films on the damping of surface waves. His model can be incorporated with the present analysis of shear-flow instability. However, we do not do so, since there are no observations available to examine quantitatively the combined theoretical model. Hence, the discussion in the

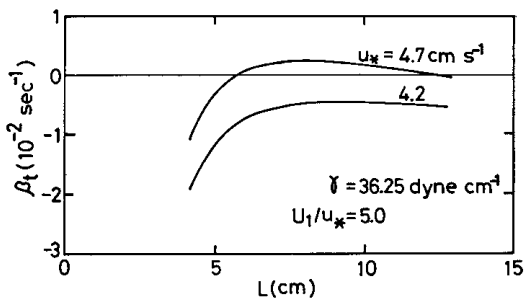

Fig. 5. Stability curves for the case of $r=5$, with a reduced value of surface tension γ.

remaining part of this paper is limited to rather qualitative arguments, based on a comparison between the growth rates predicted in Fig. 1 and the damping rates predicted by the Miles' (1967) model. In the calculation of the latter, the surface viscosity and the solubility of the surface material are neglected and the surface elasticity χ alone is considered for the sake of simplicity. Under these conditions, Miles' (1967) model predicts the temporal damping rate $-\beta_t$ of the wave amplitude, as

$$-\beta_t=\frac{1}{4}k\sqrt{2\nu_w\sigma}\frac{\zeta^2}{(\zeta-1)^2+1} \qquad (12)$$

where ζ is the nondimensional value of the surface elasticity defined by

$$\zeta=\left(\frac{1}{2}\rho_w{}^2\nu_w\sigma^3\right)^{-1/2}k^2\chi \qquad (13)$$

where k is the wave number and σ the angular frequency of waves. In the calculation, σ is determined from the dispersion relation of surface waves for the case of no mean motion in the air and water.

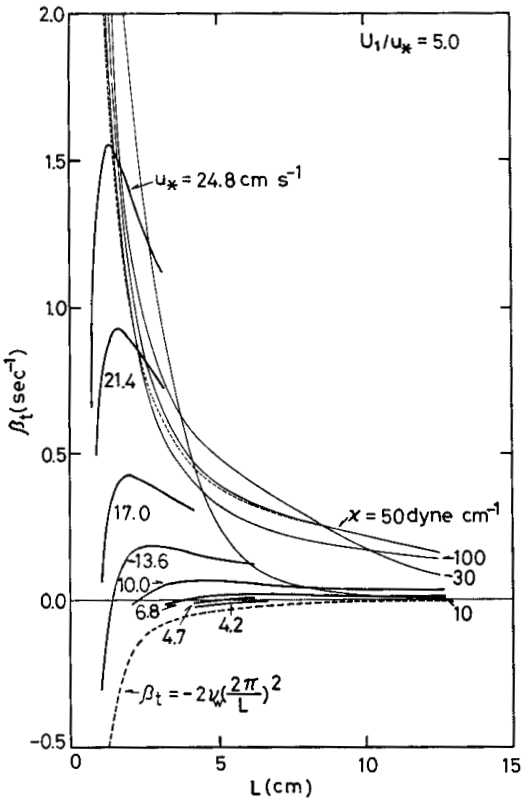

Fig. 6. Stability curves (thick solid lines) predicted in Fig. 1 and damping rates (thin solid lines) predicted by Miles' (1967) model for four possible values of surface elasticity and $\gamma=72.5$ dyne cm^{-1}. The damping rates are shown with positive sign. Thick dashed line represents the damping rates caused by the viscosity of water. Thin dashed line represents the damping rates predicted by Miles' (1967) model for $\chi=50$ dyne cm^{-1} and $\gamma=36.25$ dyne cm^{-1}.

The comparison is shown in Fig. 6, where the thick solid lines represent the growth rates predicted in Fig. 1, the thin lines the damping rates expected from Miles' (1967) model for several possible values of χ, and the thick dashed line the damping rates given by LAMB (1932) for the case of no mean motion in the air and water. For the calculation, the viscosity ν_w and the surface tension γ are taken as 0.01 cm^2 s^{-1} and 72.5 dyne cm^{-1}, respectively, and these remain equal to those of Figs. 1 to 3. For the case $\chi=50$ dyne cm^{-1}, the results with $\gamma=36.25$ dyne cm^{-1} are also shown with a thin dashed line, which reveals that the change of surface tension has no significant effect. In the figure, the values of β_t calculated by Miles' (1967) model are shown with positive sign, for the sake of easy comparison. It can be seen that the growth rates of the initial wavelets, which correspond to the waves whose growth rate is maximum for a given wind speed, as shown by KAWAI (1979), are comparable to or smaller than the damping rates caused by the surface elasticity. Hence, the initial wavelets observed by KAWAI (1979) at least are expected to disappear under the existence of surface films with these values of surface elasticity. Although the behavior of these curves for longer waves is not clear in the figure, it is also expected that the theoretical value of the critical wind speed is significantly increased in the presence of surface films. In conclusion, the increase in the actual value of the critical wind speed is presumably caused by surface films, although this statement has to be examined quantitatively on the basis of precise experiments.

Acknowledgements

The author wishes to thank Prof. K. KAJIURA of the University of Tokyo and Prof. Y. TOBA of Tohoku University for their stimulative suggestions and comments. He also thanks Mr.

P. S. JOSEPH of Tohoku University for his improvements of the wording in the manuscript. The computation contained in the present article was performed by use of ACOS-NEAC-700 at the Computer Center of Tohoku University.

References

GASTER, M. (1962): A note on the relation between temporally-increasing and spatially-increasing disturbances in hydrodynamic stability. J. Fluid Mech., **14**, 222-224.

JEFFREYS, H. (1924): On the formation of water waves by wind. Proc. Roy. Soc. London, Ser. A, **107**, 189-206.

KAWAI, S. (1979): Generation of initial wavelets by instability of a coupled shear flow and their evolution to wind waves. J. Fluid Mech., **93**, 661-703.

KEULEGAN, G. H. (1951): Wind tides in small closed channels. J. Res. Nat. Bur. Stand., **46**, 358-381.

KUNISHI, H. (1957): Studies on wind waves with use of wind flume (I)—On the shearing flow in the surface boundary layer caused by wind stress. Ann. Disas. Prev. Res. Inst., Kyoto Univ., **1**, 119-127 (in Japanese with English abstract).

KUNISHI, H. (1963): An experimental study on the generation and growth of wind waves. Disas. Prev. Res. Inst., Kyoto Univ., Bull., No. 61, 41 pp.

LAMB, H. (1932): Hydrodynamics. 6th ed. Cambridge Univ. Press, Cambridge, U. K., 738 pp.

MILES, J. W. (1957): On the velocity profile for turbulent flow near a smooth wall. J. Aero. Sci., **24**, 704.

MILES, J. W. (1962): On the generation of surface waves by shear flows. Part 4. J. Fluid Mech., **13**, 433-448.

MILES, J. W. (1967): Surface-wave damping in closed basins. Proc. Roy. Soc. London, Ser. A, **297**, 459-475.

REYNOLDS, O. (1880): On the effect of oil on destroying waves on the surface of water. Pap. Br. Assoc. Rept., **1**, 409.

ROLL, H. U. (1951): Neue Messungen zur Entstehung von Wasserwellen durch Wind. Ann. Met., **4**, 269-286.

TAKEMATSU, M. (1978): On the instability of air flow over a water surface. Rep. Res. Inst. Appl. Mech., Kyushu Univ., **25**, 167-182.

VALENZUELA, G. R. (1976): The growth of gravity-capillary waves in a coupled shear flow. J. Fluid Mech., **79**, 229-250.

VAN DORN, W. G. (1953): Wind stress on an artificial pond. J. Mar. Res., **12**, 249-276.

せん断流不安定理論に基づく風波発生の臨界風速に関する考察

河　合　三四郎*

要旨: せん断流不安定理論から予想される風波発生の臨界風速と，これに関する観測事実との比較から以下の結論を得た．臨界風速は吹送距離の関数であり，今回の理論モデルが与える吹送距離が無限大の場合の臨界風速は，水面上 30 cm の高さで 93 cm s^{-1} である．この値は吹送距離が十分大きい場合の観測値と一致した．水に石けんを加えたときに臨界風速が非常に増大するが，この増大は石けん注入による表面張力の低下によっては説明されず，石けん注入にともない形成される表面膜の効果を考慮しなければならない．表面膜の弾性だけを考慮したやや定性的な議論によれば，表面膜の存在が臨界風速の大幅な増大に効果的である．

* 東北大学理学部地球物理学教室
〒980 仙台市荒巻字青葉